Experimental study on the aeroacoustic characterization of exhaust mufflers in the presence of mean flow

B. Vanelderen, W. De Roeck, D. Vandeun, Y. Mattheys, P. Sas, W. Desmet
K.U.Leuven, Department of Mechanical Engineering,
Celestijnenlaan 300 B, B-3001, Leuven, Belgium
e-mail: **bart.vanelderen@mech.kuleuven.be**

Abstract

For the aeroacoustic design of mufflers, commonly installed in HVAC ducts, automotive exhaust systems or other confined flow applications, both the convective noise propagation and the aerodynamic noise generation mechanisms should be taken into account. An experimental procedure, based on an active two-port formulation, allows a straightforward characterization of both phenomena and gives further insight in the aeroacoustic performance of acoustic filters. This paper describes the development of such an experimental procedure which is validated for a simple rectangular expansion chamber, using an analytical reference solution. Afterwards, flow effects on the noise attenuation behavior and aerodynamic noise generation mechanisms are investigated for various muffler configurations which are of engineering relevance. The results show that the experimental approach allows to obtain a good estimation for both the attenuation and the noise generation characteristics in a frequency range from 60 to 2000 Hz and in presence of flow with a Mach number up to 0.3. As such the measurement technique offers a valuable tool for the evaluation of the filter performance and allows to generate a benchmark database which can be used for the validation of computational aeroacoustics prediction techniques.

1 Introduction

Mufflers are commonly installed in flow duct systems, such as HVAC ducts and automotive exhaust systems, to attenuate the noise emitted by upstream sound sources like internal combustion engines, fans, compressors, upstream turbulence,... Nowadays, for an ambient medium at rest, the acoustic attenuation principles are quite well understood, which has lead to the production of high-performance acoustic filters with only a minimum of additional back pressure using analytical and numerical design tools [1]. Although, the presence of a non-uniform (time-pulsating) mean flow and of strong thermal gradients can significantly influence the acoustic properties of muffler, their effects can only be taken limited into account by these design methodologies. For this reason, new numerical approaches are emerging [2]. However, these methods are, at present, only applicable for problems with moderate geometrical complexity and experimental data are indispensable for the validation of these new design tools.

With the recent advancements in quiet engine technology and the reduction of fan noise sources, a second phenomenon is becoming of increasing importance for the acoustic design of mufflers. It is the aerodynamic noise generation that becomes more pronounced at medium and high engine speeds and can even become the dominant source of exhaust noise [3, 4]. In this framework, expansion chambers can become flow-excited noise generators rather than silencers. This aeroacoustic noise generation contains broadband and tonal components caused by, respectively, the turbulent structures inside the ducts and muffler; and the broadband excitation of the acoustic modes or the occurrence of a

flow-acoustic feedback coupling. Computational AeroAcoustics (CAA) methodologies to study these noise sources are, at present, too computationally demanding and, as a result, not yet competitive to an experimental measurement campaign.

Thus, it is clear that for the aeroacoustic design of mufflers both the aerodynamic noise generation and propagation characteristics are of utmost importance, aiming at a maximal sound attenuation in the downstream direction with only a minimum amount of additional flow noise generation. Since it is not possible to accurately analyze the aeroacoustic behavior of mufflers of engineering complexity using state-of-the-art CAA tools, experimental procedures to determine the aeroacoustic properties of these devices are indispensable. Therefore, the goal of this paper is the development and validation of an experimental methodology, based on an active two-port formulation, for the characterization of acoustic filters in the presence of a non-uniform mean flow.

The experimental active two-port formulation is validated for a simple rectangular expansion chamber with a quiescent medium and a 'artificial' narrowband internal noise production, generated using a loudspeaker mounted on top of the expansion chamber. For engineering applications, a simple expansion chamber is not fully representative since typical muffler configurations have an cylindrical or elliptical geometry and contain a large number of internal components such as rigid and perforated pipes; baffles and sound absorbing materials. For this reason, the active two-port characterization is applied to six different cylindrical muffler configuration which contain one or more of these internal components and with different Mach numbers (M) of the mean flow field. The test objects, that are studied in this paper, are of thus of engineering relevance but with a moderate geometrical complexity. As such, the experimental results can be used as a benchmark database for the validation of different CAA methodologies.

The outline of this paper is the following: in the next section the flow acoustic test facility and the different muffler geometries are described. Subsequently, the experimental procedure to determine the active two-port characteristics is given in further detail. Section 5 discusses , at first, the validation of the experimental procedure for a simple rectangular expansion chamber. Afterwards, the attenuation and aerodynamic noise generating characteristics of the various muffler configurations are investigated. The major conclusions, drawn from this analysis, are summarized in the final section. The results, that are presented in this paper, are preliminary in the sense that they are mainly used to characterize the test rig performance. Based on the outcome of this paper, the limitations of the test rig and the experimental procedure are identified and modifications of the current test facility are suggested. Future research will focus on a more accurate determination of the two-port characteristics. It should also be mentioned that the analysis, presented in this paper, is limited to only aeroacoustic effects. For an efficient and useful design of an acoustic filter, other aspects, specifically a minimum of additional back pressure generation, should be taken into account.

2 Description of the test facility and test objects

2.1 Flow-acoustic test rig

For the measurements, shown in this paper, an open-circuit aeroacoustic test rig (Fig. 1) is used [5]. The general purpose of the test rig is the determination of the aeroacoustic noise generation and propagation mechanisms (including active two-port characterization and grazing flow impedance eduction measurements) as well as the far field acoustic radiation (not used in this paper) for confined, subsonic flow applications with inflow conditions that are representative for HVAC and automotive muffler applications. The test facility can be divided in three different components: the flow generation part, the measurement section and the test object.

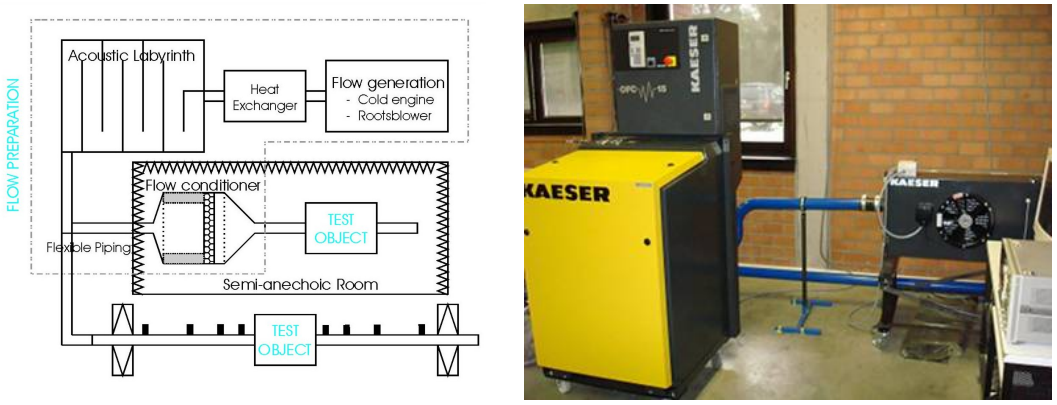

Figure 1: Schematic overview of aeroacoustic test set-up (left), rootsblower with aftercooler (right)

2.1.1 Flow generation

Two flow generators can be used: a rootsblower, shown on the right of figure 1, to generate a time-uniform flow field or a cold engine simulator for future experiments with time-pulsating flow fields. The rootsblower has three lobes to minimize both noise generation and small time-pulsations of the flow. A frequency regulator with PID controller, coupled with downstream pressure and flow rate sensors, is attached to the rootsblower in order to ensure identical inlet conditions between different measurement campaigns. The maximum Mach number that can be achieved equals 0.35 for duct diameters equal to $0.05\,m$. Both the duct diameter and maximum Mach number are representative for automotive exhaust system applications. The rootsblower's air compression is responsible for an increase in temperature of more than $60^o\,C$. For this reason, an aftercooler is installed immediately after the rootsblower, generating an outlet temperature of the compressed air of $5^o\,C$ above the ambient temperature with temperature fluctuations less than 2.5% between different measurement campaigns. After the heat exchanger the flow can be guided through an acoustic labyrinth and flow conditioner inside a semi-anechoic room where aerodynamic flow visualization (using e.g. particle image velocimetry) or far field acoustic radiation measurements can be carried out; or, as discussed in this work, the flow immediately enters the measurement section of the acoustic propagation test rig.

2.1.2 Measurement section

The measurement section consists of two straight ducts with a length (L) of $2.5\,m$, and a square cross section ($40 \times 40\,mm^2$), between which the test objects can be placed (left of Fig. 2. Each measurement duct contains five flush-mounted dynamic pressure transducers (type: *PCB 106B*). The approximate distances between the different pressure transducers and the test object are, respectively, $35\,mm$, $116\,mm$, $247\,mm$, $459\,mm$ and $2400\,mm$. At the end of each measurement section an in-line loudspeaker is installed (right of Fig. 2). In front of the upstream measurement duct a vortex-flowmeter is installed to accurately determine the flow rate which enters the test object. It should be mentioned that for all measurements, the same square cross section of the measurement duct has been used. For the various cylindrical muffler configurations, which have a circular cross section of the inlet and outlet duct, a small ($L = 200\,mm$) connection duct has been used. Since the goal of this paper is a validation of the experimental test facility and the measurement procedure, rather than obtaining an accurate estimation of the two-port characteristics of the muffler 'proper'; the performed measurements have not been corrected for this connecting piece and, as a result, they will be slightly influenced by the presence of these transition pieces. In future research, a round measurement section will be used to eliminate these effects.

Figure 2: Picture of the flow-acoustics test rig (left) and an in-line loudspeaker (right).

2.2 Description of the test objects

2.2.1 Rectangular expansion chamber

The simple rectangular expansion chamber, which is used to validate the experimental active two-port determination technique is shown in figure 3. It consist of a simple rectangular expansion chamber ($L = 225\,mm$) with square ($120 \times 120\,mm^2$) cross section. The inlet and outlet ducts have an identical, square, cross section ($40 \times 40\,mm^2$) as the measurement duct on which the pressure sensors are mounted. On the top of the expansion chamber an additional loudspeaker (shown on the right of Fig. 3) is installed in order to artificially simulate an internal noise generation which is representative for the aerodynamic noise generation, occurring inside expansion chamber type of geometries. The experiments that are carried out for this test object are all performed under quiescent conditions and are mainly used to validate and propose small improvements to some aspects of the experimental characterization procedure which are related to the data acquisition, the experimental set-up and the data processing.

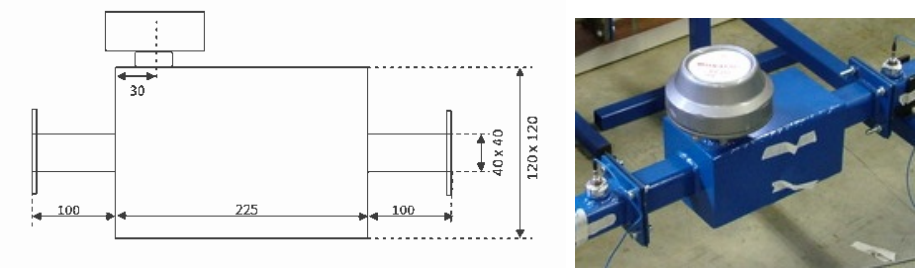

Figure 3: Geometry of the rectangular expansion chamber.

2.2.2 Mufflers of engineering complexity

After the validation of the experimental procedure for the simple rectangular expansion chamber, the active two-port characterization methodology is applied to six different muffler configurations, containing a number of different internal components, thus making them more relevant for engineering muffler applications in comparison to the simple rectangular expansion chamber. The various muffler configurations are shown in figures 4 and 5. The cross section of the inlet and outlet pipes off all mufflers are circular with a diameter equal to $40\,mm$. As mentioned before, this has as a consequence that additional connection pieces are needed to mount the test objects onto the measurement ducts which can influence the two-port parameters. In order to avoid structural vibrations

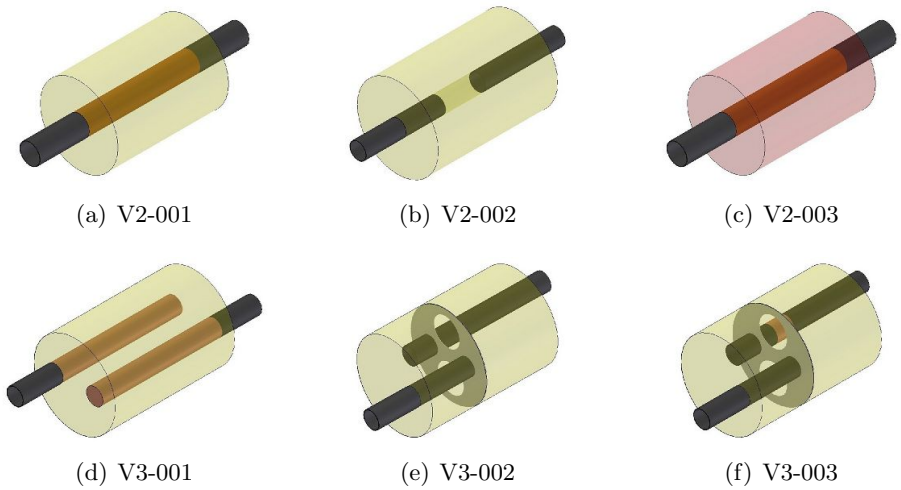

(a) V2-001 (b) V2-002 (c) V2-003

(d) V3-001 (e) V3-002 (f) V3-003

Figure 4: Graphical representation of various muffler configurations.

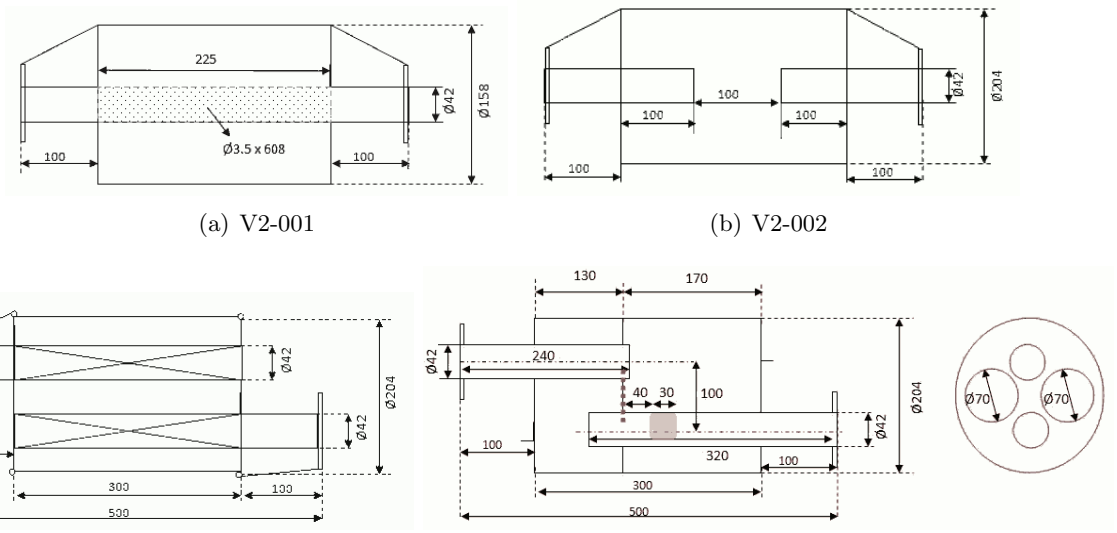

(a) V2-001 (b) V2-002

(c) V3-001 (d) V3-003

Figure 5: Geometrical parameters of the various muffler configurations.

and their possible influence on the noise attenuation and aerodynamic noise generating characteristics, additional stiffening bars (Fig. 5) are installed on most the the muffler configurations.

The various muffler configurations can be divided into two categories:

- The first category ($V2$) contains mufflers where the centerline of both the inlet and outlet ducts are coincident with the centerline of the expansion chamber.
- For the mufflers belonging to the second category ($V3$), the centerlines of the inlet duct, expansion chamber and outlet duct are coplanar, with a positive and negative offset of $50\,mm$ between the centerlines of the expansion chamber and, respectively, the inlet and outlet duct.

The difference between the different muffler geometries is characterized by a gradual increase in geometrical complexity:

- For muffler $V2-001$, the inlet and outlet duct are connected with perforated duct containing 608 perforates with a diameter equal to $3.5\,mm$, leading to a porosity of 19.7%).

- Muffler $V2-002$ is and extended inlet-extended outlet expansion chamber with an equal extension of $100\,mm$ for both the inlet and outlet duct.
- The geometrical parameters of muffler $V2-003$ are identical to muffler $V2-001$ but the expansion chamber, surrounding the perforated pipe, is filled with a specific type of glass wool.
- For muffler $V3-001$, the inlet and outlet duct are extended to back, respectively, front of the expansion chamber using a perforated duct with 7129 perforates with a diameter equal to $1.015\,mm$, leading to a porosity of 19%).
- Muffler $V2-002$ is an extended inlet-extended outlet type of muffler with an additional baffle structure, separating the exit of the inlet duct form the entrance of the outlet duct. In contrast to commonly used baffle structures, which typically contain a large number of small diameter perforates, the connection between the front and the back of the expansion chamber is constructed using two large holes with a diameter of $70\,mm$. This is mainly chosen to facilitate the possibility to simulate the aeroacoustic behavior of this muffler configuration in future CAA-research.
- Muffler $V2-003$ is identical to muffler $V2-002$ with the exception of an additional perforated section ($L = 30\,mm$) in the extension of the outlet duct behind the baffle.

The main properties of the different test objects are summarized in table 1.

Name	Chamber length	Chamber diameter	Perforates	Glass wool	Baffle	Offset
$V2-001$	$225\,mm$	$158\,mm$	yes	no	no	no
$V2-002$	$225\,mm$	$204\,mm$	no	no	no	no
$V2-003$	$225\,mm$	$158\,mm$	yes	yes	no	no
$V3-001$	$300\,mm$	$204\,mm$	yes	no	no	yes
$V3-002$	$300\,mm$	$204\,mm$	no	no	yes	yes
$V3-003$	$300\,mm$	$204\,mm$	yes	no	yes	yes

Table 1: Properties of the various muffler configurations

3 Experimental active two-port characterization

Acoustic systems, located between two straight ducts in which acoustic plane wave propagation is occurring, are often referred to as acoustic two-ports [1] (Fig. 6). Every acoustic two-port is uniquely characterized by an acoustic transfer matrix $\mathbf{T}$ also known as the transmission matrix, scattering matrix or four-pole parameter representation, coupling the acoustic variables (e.g acoustic pressure and velocity fluctuations) at the inlet (1) and outlet (2) of the acoustic element.

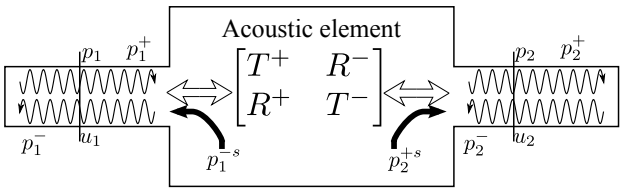

Figure 6: Graphical representation of an acoustic two-port and scatter matrix.

One of the most commonly used representations of the transfer matrix is using the pressure of the right- and left-running acoustic waves (p^+, p^-) (instead of the pressure and velocity fluctuations) at

both ends of the two-port. In this way, the four matrix elements T^+, T^- and R^+, R^- can be directly interpreted physically as the transmission and reflection coefficients in, respectively, the downstream and upstream direction. If non-linear active noise generation and/or dissipation processes occur inside the filter, an active two-port representation can be used by adding two additional source terms in the downstream and upstream direction (p_2^{+s}, p_1^{-s}), the active two-port parameters [6]. This leads to following matrix formulation:

$$\left\{ \begin{array}{c} p_2^+ \\ p_1^- \end{array} \right\} = \left[\begin{array}{cc} T^+ & R^- \\ R^+ & T^- \end{array} \right] \left\{ \begin{array}{c} p_1^+ \\ p_2^- \end{array} \right\} + \left\{ \begin{array}{c} p_2^{+s} \\ p_1^{-s} \end{array} \right\} \tag{1}$$

The passive two-port components (four-pole parameters) T^+, T^-, R^+ and R^- are independent of the internal or external noise generation mechanisms and the upstream and downstream impedance. As such, they describe the 'filter proper'. Opposite to these components, the active noise generation components in the downstream p_2^{+s} and upstream direction p_1^{-s} can be dependent on the upstream and downstream impedance [7].

Although the acoustic element is treated as a 'black-box', the active two-port formulation is a very useful tool for the aeroacoustics analysis of flow duct systems with potential applications of a.o.:

- The determination of the **propagation characteristics**: The passive two-port coefficients offer direct information about the noise propagation principles of an acoustic filter. Performance parameters such as e.g. the transmission loss ($TL = 20\log(1/T^+)$) can be derived from the scatter matrix coefficients. Furthermore, physical properties such as a reciprocal behavior and acoustic energy conservation can be directly deduced from the matrix coefficients [8].

- The **characterization of acoustic absorbent materials** in the presence of a non-uniform mean flow: When the, experimentally obtained, transfer matrix coefficients are compared to analytical or numerical reference models material properties such as e.g. the grazing flow acoustic impedance can be deduced [9].

- The **aeroacoustic design of duct networks**: Since passive two-port models are independent of the upstream and downstream impedance (i.e. independent of the acoustic properties of the pre- and ante-ceding elements) various design alternatives can easily be evaluated, using only simple matrix multiplications, resulting in a low CPU-cost design tool, provided that the different elements are present in a 'network database' [1].

- The identification of **flow-acoustic feedback coupling**, i.e. the possible existence of unstable (tonal) 'whistling' phenomena: Since this phenomenon is (initially) caused by a linear interaction of the incoming waves with the aerodynamic field, these effects are present in the scatter matrix coefficients. Although, due to non-linearities, it is not possible to predict the 'exact' (limit cycle) acoustic field inside a flow duct, the occurrence possible instabilities can be identified using an eigenvalue decomposition of the linear active two-port matrices [10].

- The **quantification of aerodynamically driven flow-noise generation mechanisms**: It is possible to obtain spectral information about the upstream and downstream radiated aeroacoustic field and its Mach number dependency without the need of detailed information about the actual noise generating mechanisms [5].

The different active two-port matrix coefficients can be easily obtained analytically [1], experimentally [11, 12] or numerically [13]. The experimental determination of the active two-port parameters consists in three steps:

1. The determination of the amplitudes of the upstream and downstream propagating waves at both ends of the acoustic two-port: p_1^+, p_1^-, p_2^+ and p_2^-

2. Characterization of the scattering matrix coefficients (passive two-port components): T^+, T^-, R^+ and R^-

3. Determination of the active source vector components: p_2^{+s} and p_1^{-s}

3.1 Upstream and downstream propagating waves

For the determination of the upstream and downstream propagating waves (p^+,p^-) at each end of the two-port, the dynamic pressure sensor signals at a minimum of two positions are needed in the measurement duct. The left- and right running amplitudes are directly linked to the acoustic velocity and pressure fluctuations, since at any location z in the duct the following relation holds for plane acoustic wave propagation:

$$p'(z,f) = p^+(z,f) + p^-(z,f) = p^+(0,f)e^{-jk^+z} + p^-(0,f)e^{jk^-z} \tag{2}$$

with $z = 0$ the position of the reference plane and $k^+ \approx k_0/(1-M)$ and $k^- \approx k_0/(1+M)$ the acoustic wavenumbers of, respectively the downstream and upstream propagating waves and $k_0 = \omega/c_0$. For non space-uniform mean flows a more accurate formulation for k^+ and k^- can be obtained using a quasi 2D approach [14]. Equation (2) can be written for all n microphone positions and solving following overdetermined system of n equations with two unknowns, resulting in a solution for p^+ and p^- at both ends of the two-port:

$$\left\{ \begin{array}{c} p^+(f) \\ p^-(f) \end{array} \right\} = \left[\begin{array}{cc} e^{-jk^+z_1} & e^{jk^-z_1} \\ e^{-jk^+z_2} & e^{jk^-z_2} \\ \vdots & \vdots \\ e^{-jk^+z_n} & e^{jk^-z_n} \end{array} \right]^{\otimes} \left\{ \begin{array}{c} p'(z_1,f) \\ p'(z_2,f) \\ \vdots \\ p'(z_n,f) \end{array} \right\} \tag{3}$$

with $\bigotimes$ the Moore–Penrose pseudo matrix inverse and z_k the location of the k^{th} microphone with respect to the reference plane. The overdetermination of this system of equations is desired improve the signal-to-noise ratio and to minimize the influence of aerodynamic pressure fluctuations. Since the aerodynamic pressure fluctuations, present in the microphone signals, do not satisfy equation (3) they are partially filtered out by these equations. A further improvement of the signal-to-noise ratio is achieved by using a large number of averages and transfer functions in equation (3) instead of the measured pressure fluctuations. These transfer functions are taken between the microphone signals and a reference signal which is correlated with the acoustic field inside the duct. In this sense the electric signal e which drives the external loudspeaker is a convenient choice. For clarity reasons, the notation, used in this paper, still uses the pressure fluctuations of the k^{th} measurement: $p_k(f)$ instead of the transfer function $H_k(f) = p_k(f)e^*(f)/e(f)e^*(f)$ (with $\bullet^*$ the complex conjugate).

3.2 Passive two-port characteristics

In order to determine the two-port matrix coefficients, at least two measurements need to be performed varying from each other by the position of an external sound source (two-source technique) [11, 12], by the outlet impedance (two-load technique) [15] or a combination of both techniques. Equation (1) can then be written for m experiments without active components, since with a strong enough loudspeaker excitation the aerodynamic noise generation can be neglected ($p_2^{+s} = p_1^{-s} \approx 0$). As a result a combined overdetermined system of m equations with four unknowns T^+, T^-, R^+ and R^- is obtained, which can be solved following a least square strategy:

$$\begin{bmatrix} T^+(f) & R^-(f) \\ R^+(f) & T^-(f) \end{bmatrix} = \begin{bmatrix} p^+_{2,1}(f) & p^+_{2,2}(f) & \dots & p^+_{2,m}(f) \\ p^-_{1,1}(f) & p^-_{1,2}(f) & \dots & p^-_{1,m}(f) \end{bmatrix} \begin{bmatrix} p^+_{1,1}(f) & p^+_{1,2}(f) & \dots & p^+_{1,m}(f) \\ p^-_{2,1}(f) & p^-_{2,2}(f) & \dots & p^-_{2,m}(f) \end{bmatrix}^{\otimes} \tag{4}$$

3.3 Determination of the active source vector

Opposite to the passive two-port components, the active noise generation components in the downstream p_2^{-s} and upstream direction p_1^{+s} are dependent on the upstream and downstream impedance [7]. As a result, an overdetermined system of equations, using a different impedance at the inlet or outlet section, cannot be used for the determination of the active source vector components. Also multiple sources techniques cannot be used since they can mask the actual aerodynamically generated noise, resulting in a low signal-to-noise ratio. Thus, the active two-port parameters have to be obtained experimentally (for one specific combination of inlet and outlet impedance) with one additional measurement without loudspeaker excitation and solving a system of two equations (1) for the two unknowns (p_2^{+s}, p_1^{-s}) using the previously determined passive two-port parameters.

$$\begin{bmatrix} p_2^{+s} \\ p_1^{-s} \end{bmatrix} = \begin{bmatrix} p_2^{+} \\ p_1^{-} \end{bmatrix} - \begin{bmatrix} T^+ & R^- \\ R^+ & T^- \end{bmatrix} \begin{bmatrix} p_1^{+} \\ p_2^{-} \end{bmatrix} \tag{5}$$

As reference signal, for the determination of the different transfer functions, two additional microphones are used which are located at further distance from the inlet and outlet reference planes. The aerodynamic pressure fluctuations in this region are uncorrelated with those measured by the other microphones and, as a result, a further suppression of these non-acoustical disturbances is achieved.

4 Experimental set-up

A schematic overview of the experimental set-up is shown in figure 7. As excitation signal, a series of swept sines (sweep duration: $1\,s$; frequency range: $0-4000\,Hz$) are used for a measurement time of $300\,s$. The data acquisition is carried out using the *LMS international Pimento Multi Channel Analyzer* with a sample frequency of $10\,kHz$. The data are averaged using, approximately 1000 averages with an overlap of 25%. Four different flow velocities are used for the various muffler configurations: $M = 0.0$; $M = 0.1$, $M = 0.2$ and $M = 0.3$ with exception of the rectangular expansion chamber, which is only analyzed for the no flow case.

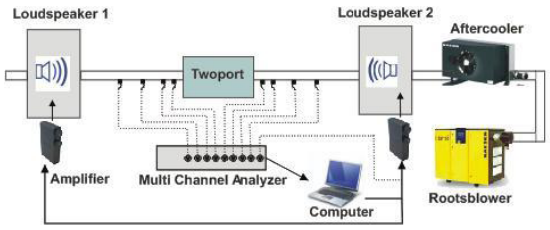

Figure 7: Schematic overview of the experimental set-up

For the passive two-port characterization, a combined two-load/two-source approach is used, resulting in a total number of four measurements per muffler and per flow velocity. As different loads a rigidly closed and open end termination is used for the no flow cased whereas an open end and a downstream installed muffler are used for the measurements which include the presence of a

flow. The pressure sensors are calibrated using a hand-held acoustic microphone calibrator. The exact locations of the microphone positions are determined for each measurement section up to an accuracy of $0.1\,mm$ with a swept sine excitation and a rigid wall termination. Using the transfer functions between the different microphones, the exact location is easily obtained since the transfer functions show a first minimum or maximum for each microphone when the distance between the rigid termination equals 1/4 of the acoustic wavelength [16].

The first traversal mode of the $40 \times 40\,mm^2$ square measurement section occurs at approximately $4125\,Hz$. Since a two-port formulation is only valid for plane wave propagation, the results are discussed up to a frequency of $3400\,Hz \approx 0.8 \times 4125\,Hz$ for the rectangular expansion chamber and up to $2000\,Hz \approx 0.5 \times 4125\,Hz$ for the other muffler configurations. Future research will study in further depth the acoustic behavior of the various muffler configurations in the frequency range between $2000\,Hz$ and $3400\,Hz$.

5 Discussion of the results

5.1 Rectangular expansion chamber

5.1.1 Scatter matrix coefficients

The rectangular expansion chamber (Fig. 3) is considered for validating the experimental determination of the passive scatter matrix coefficients and in particular the data acquisition settings and the data processing using an overdetermination of the number of microphones (eq. (4)) and the number of measurements (eq. (3)). The results are compared with an analytical reference solution obtained by using Green's functions [17]. This approach offers an exact analytical solution, apart form the necessary truncation of the in finite sum of modal contributions. A comparison between the four, experimentally obtained, scatter matrix coefficients and the analytical solution is shown in figure 8. A very good agreement between both predictions is observed for all matrix coefficients and over the whole frequency range under consideration, indicating that the methodology offers a reliable prediction of the acoustic behavior of the expansion chamber under no flow conditions.

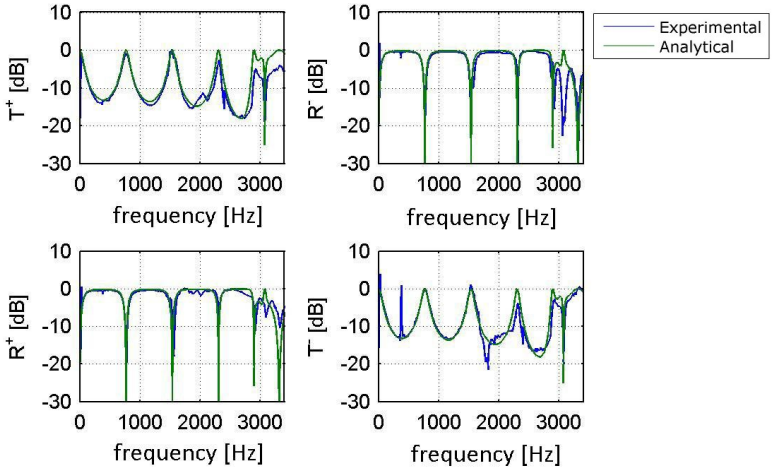

Figure 8: Comparison between the measured and analytical scatter matrix coefficients (dB) for the rectangular expansion chamber.

5.1.2 Active source vector determination

The active source vector determination is validated by adding an artificial noise source, using a loudspeaker excitation, inside the expansion chamber. The excitation signal contains both broadband ($500 - 900\,Hz$) and tonal noise components (600, 1200 and $1800\,Hz$) and is shown in figure 9. Since the artificial noise source is independent on the incoming acoustic wave, a similar spectrum should be observed in the active source vector components. This is clearly noticeable in figure 9, indicating that the active two-port representation is capable in retrieving internal noise source of the acoustic element which are independent on the incoming acoustic waves. The slight difference between the upstream and downstream components of the active source vector is caused by the non-symmetric position of the central loudspeaker (Fig. 3).

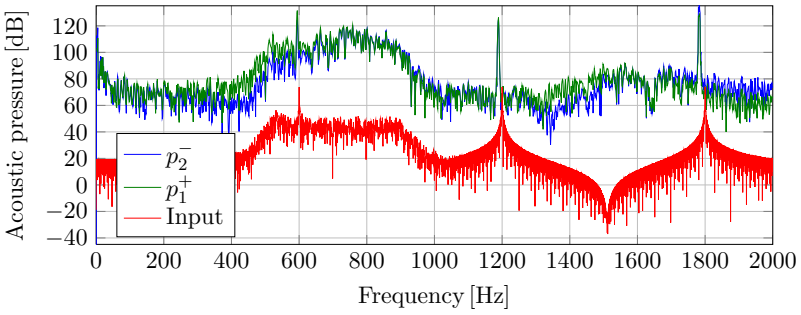

Figure 9: Active source vector components in upstream and downstream direction (dB) and loudspeaker excitation signal for the rectangular expansion chamber.

5.2 Mufflers of engineering relevance

The same approach as used for the rectangular expansion chamber is applied to the different muffler configurations which contain components that are of engineering relevance (Fig. 4). The measurements are carried out at three different Mach number corresponding to 0.0 (no flow), 0.1, 0.2 and 0.3. For the active source vector determination, no external loudspeaker signal is used since the goal is the predict the actual aerodynamic noise radiation in the upstream and downstream directions.

5.2.1 Transmission characteristics

The transmission loss (TL), which is, as mentioned above, directly related to the downstream transmission coefficient of the scatter matrix, for the different muffler configurations and Mach numbers is shown in figure 10 for frequencies up to $2000\,Hz$. For mufflers $V2 - 001$, $V2 - 002$ and $V3 - 001$ a comparison is made with a (no flow) finite element solution, obtained with *Sysnoise rev.:5.6*. For this reference solution, the perforated ducts are modeled using transfer matrix relation and the impedance formula for perforates in an stationary medium of Sullivan and Crocker [18].

In general, for the no flow case, a good agreement between the numerical simulations and the experimental values of the transmission loss. However, in the frequency range between $250\,Hz$ and $400\,Hz$ a systematic overprediction of the TL with approximately $7\,dB$ is noticeable. This is caused by the presence of the connection pieces between the round cross section of inlet and outlet duct of the mufflers and the square cross section of the measurement section. This was verified (not shown in this paper) by performing an additional TL measurement using only the connection pieces. The TL values that were obtained in this way, indeed exhibit an increased value of the TL in this frequency range. The errors in the TL prediction, originating from these connection ducts, can be removed by using circular measurement sections or by compensating for the connection pieces using a matrix

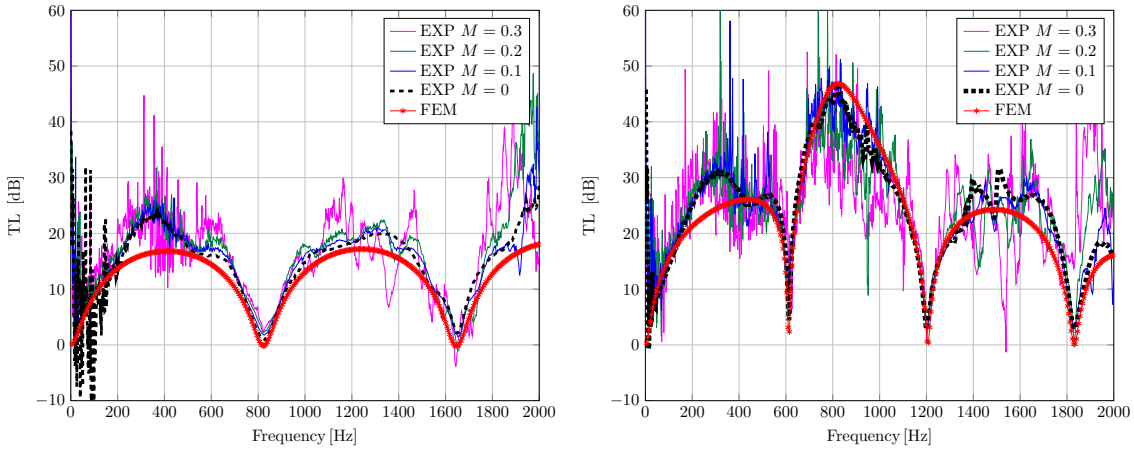

(a) V2-001

(b) V2-002

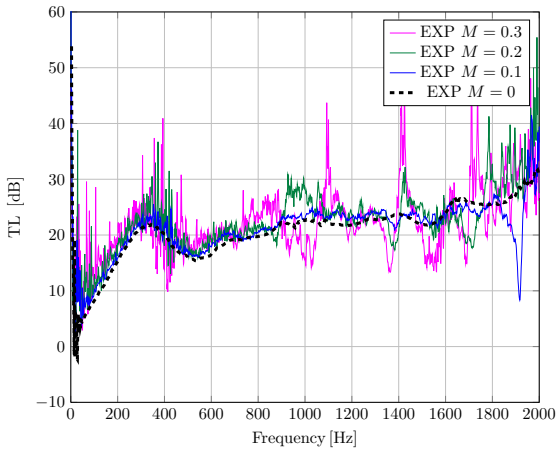

(c) V2-003

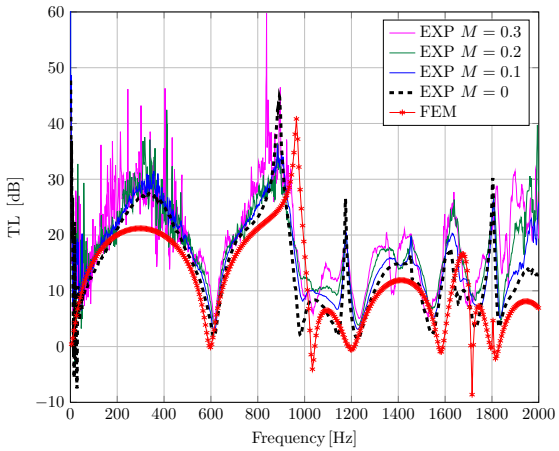

(d) V3-001

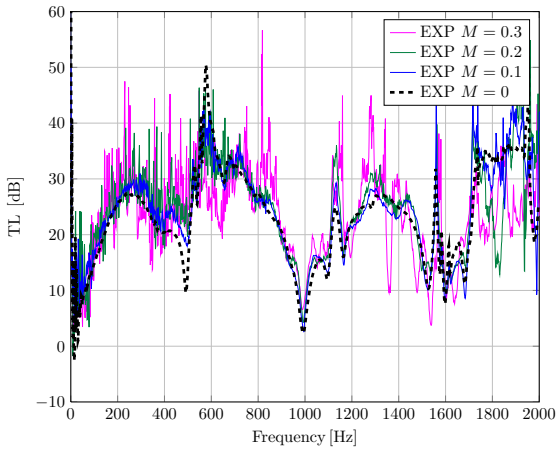

(e) V3-002

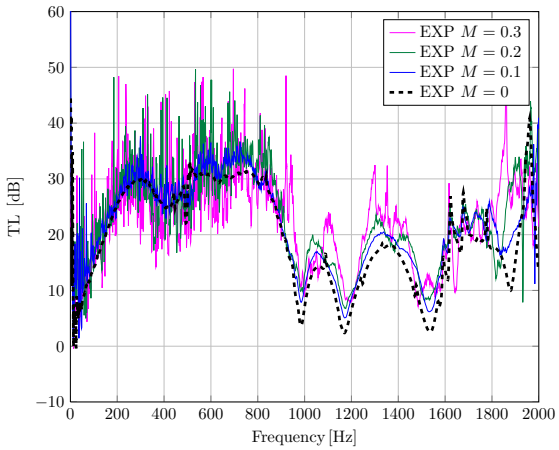

(f) V3-003

Figure 10: Transmission loss (dB) of the various muffler configurations with different values of the Mach number.

multiplication with the scatter matrices of the connection ducts. This will be investigated in future research.

At high flow velocities ($M > 0.2$), a large amount of additional noise is present in the TL predictions, mainly occurring at lower frequencies (below $900\,Hz$), high values of the TL and for mufflers with a strong turbulent outflow ($V2-002$, $V3-002$ and $V3-003$). The reason for this to occur is twofold. High TL values are, on the one hand, responsible for low-amplitude signals at the pressure sensors located on the unexcited measurement section of the acoustic two-port. This strongly decreases the signal-to-noise ratio, which is furthermore already reduced by the presence of the flow field inside the measurement ducts. The turbulent flow field in the measurement section, on the other hand, causes so-called hydrodynamic pressure fluctuations or 'pseudo-sound'. Since, these pressure fluctuation propagate with the mean flow velocity, their effect is mainly noticeable at lower frequencies and is more dominant at high flow velocities. Future research will investigate the use of a larger amount of averages; different types of excitation signals; an improvement in the pressure sensor placeholders; and the use of other types of dynamic pressure transducers to improve the signal-to-noise ratio at the different microphones and to obtain a more accurate scatter matrix prediction.

The position of the resonance frequencies at which a zero TL is obtained, does not significantly change with the presence of a mean flow. This is due to the fact that the large expansion ratios (between 16 and 25) of the muffler geometries result in very low space averaged velocities inside the expansion chamber and thus a very limited shift of these frequencies. Convective effects rather seem to influence the regions where a maximum value of the TL is obtained. For most configurations, a slight increase in TL is observed with growing flow velocities. This conclusion, however, cannot be fully evidenced since, as mentioned before, the interpretation of the experimental data at high TL is difficult due to the 'noisy' signals. For an in-depth analysis of the influence of a flow field on the attenuation performance of mufflers an accurate prediction of the frequency regions where the TL is high is indispensable, especially since this region is, from a design point of view, the most import region.

When comparing the TL of the different muffler configurations, it is clear that the presence of acoustic absorbent materials ($V2-003$) results in a good performance over the whole frequency range, as such, they are ideally suited for broadband applications and acoustic materials and applications which are not prone to a degradation of the absorbent properties of the acoustic material. For tonal or narrowband applications, as e.g. encountered in automotive applications, they do not exhibit a significant peak performance and the geometrical mufflers are possibly superior, especially at lower frequencies, where a large thickness of acoustic absorbent material is needed to obtain a significant noise reduction. It should be mentioned that although adding geometrical complexity to the muffler configuration improves the acoustic attenuation, it will also, most likely, increase the back pressure, thus decreasing e.g. the I.C. engine performance. As a result, the choice of an appropriate muffler configuration is often a compromise between maximum acoustic attenuation and a minimal back pressure.

5.2.2 Aerodynamic noise generation

Based on the scatter matrix coefficients, discussed above, an additional measurement is carried out to obtain the active source vectors. For all muffler configurations a broadband spectrum of the source vector components is observed with an overall increase in amplitude with growing Mach number. Only for muffler $V2-001$ a high-amplitude whistling frequency is observed at a frequency close to $3500\,Hz$, which is outside the frequency range of the current analysis and, as a result, this phenomenon is not discussed in this paper. The upstream and downstream source vector components exhibit a very similar frequency content with a larger amplitude of the downstream component, indicating a preferable radiation direction of the aeroacoustic sources in the downstream direction.

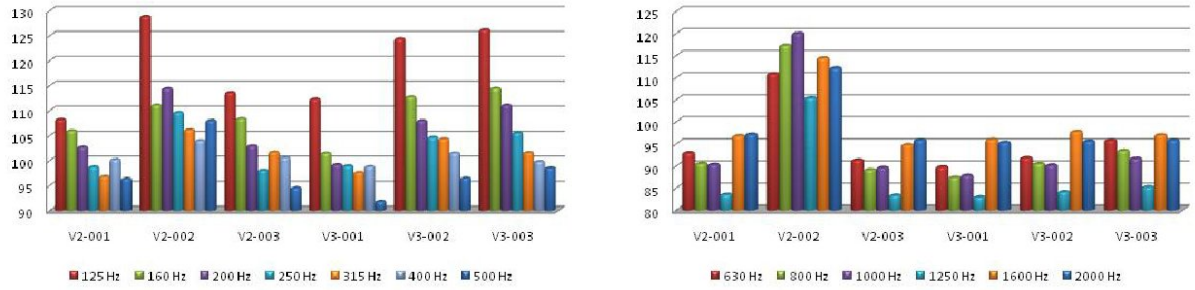

(a) 125 Hz to 500 Hz third octave bands

(b) 630 Hz to 2000 Hz third octave bands

Figure 11: Frequency spectrum (in third octave bands) of the downstream component (dB) of the active source vector for the various muffler configurations (M=0.3).

Given the broadband nature of the spectrum of the source vector and since the downstream component is dominant and more relevant for the aeroacoustic design of mufflers, a third octave band analysis is performed for only the downstream component of the active source vector. The results for the various muffler configurations are shown in figure 11 for a mean flow Mach number equal to 0.3. For the other flow velocities, similar figures are obtained.

For all muffler configurations a decrease of aerodynamic noise generation for higher frequencies is observed, with exception of the third octave bands with center frequencies of 1600 Hz and 2000 Hz where a systematic increase of aerodynamic noise generation can be noticed. This is probably caused by the presence of the connection duct between the inlet and outlet ducts and the measurement ducts but this assumption needs to be confirmed by future research. The muffler configurations with sharp edges (mufflers $V2-002$ $V3-002$ and $V3-003$) have a larger amount of flow noise generation, since the sudden detachment of the flow results in strong mean flow gradient and, as a result, a larger amount of turbulence generation.

The presence of acoustic absorbent materials (muffler $V2-003$) or a baffle (mufflers $V3-002$ and $V3-003$), which divides the expansion chamber in different components, reduces the flow noise generation. This is caused by the fact that the generated aeroacoustic sources are already partly damped out by the acoustic dissipation of the acoustic absorbent material or the geometrical reflections of the second chamber component. For mufflers $V3-002$ and $V3-003$, strong mean flow gradients occur at the exit of the inlet duct inside the downstream end of the expansion chamber, these large amplitude flow noise sources are partly damped out by the upstream part of the expansion chamber, which is especially the case for higher frequencies. Due to the lower flow velocities through the baffle holes, the additional aerodynamic noise generation is of low amplitude, which explains the relatively good aeroacoustic behavior of these mufflers. It can thus be concluded that adding geometrical complexity to the muffler by introducing sharp edges or a flow reversal to improve the acoustic attenuation, does not necessarily results in an increase in aerodynamic noise generation.

6 Conclusions

In this paper, an experimental characterization technique for acoustic filters in general, and automotive muffler applications in particular, based on an active two-port formulation is presented and validated on various muffler configurations. The experimental procedure uses an overdetermination of the number of microphones and the number of experiments to increase the signal-to-noise ratio for the prediction of the scatter transfer characteristics in the presence of a mean flow field. An additional measurement can be be carried out to determine, in combination with the previously obtained

scatter matrix coefficients, the radiation of aeroacoustic source in the upstream and downstream direction. This approach is successfully validated for a simple rectangular expansion chamber with no flow and an artificial loudspeaker excitation.

The two-port characterization procedure is applied for four different flow velocities to six muffler configurations which contain a number of internal components that are of engineering relevance such as absorbent materials, extended inlet and outlet ducts, perforated ducts and baffles. At first the most commonly design parameter for an acoustic filter, the transmission loss is considered. The results that are obtained for the no-flow case are in good agreement with numerical finite element solutions, except for a small frequency range where the specific construction of the experimental test rig causes an overestimation of approximately $7\,dB$. The influence of the flow velocity on the acoustic resonance at which a zero TL is occurring is negligible and the signal-to-noise ratio need to be further improved to draw final conclusions on the influence of the flow speed in the regions where a high value of the TL is observed.

The second aspect that needs to be taken into account in the aeroacoustic design of an acoustic filter is the aerodynamic noise generation, represented in an active two-port formulation's source vector. For the studied muffler configurations a broadband flow noise generation with a preferable downstream radiation is observed in the frequency range under consideration. Aerodynamic noise generation is of growing importance with increasing flow velocities and can be partly damped out by the different interior components of the muffler, such as sound absorbing materials and a partitioning of the expansion chamber. As a result adding geometrical complexity to a given muffler configuration can improve both the acoustic attenuation and aerodynamic noise generation properties.

Future research will focus on a further improvement of signal-to-noise ratio by considering other excitation signals, microphone placeholders and types of microphones and by optimizing the data processing. Based on these findings, it is expected that more accurate scatter matrix and active source vector predictions will be obtained for the various muffler configurations. These results will be used for the generation of an benchmark database for the validation of future computational aeroacoustics simulation. As such, a reliable and straightforward experimental methodology is developed which can be used for the aeroacoustic design and the development of a numerical prediction tool for acoustic filters.

Acknowledgements

The research of Bart Vanelderen is funded by a personal fellowship of the Institute for the Promotion of Innovation through Science and Technology in Flanders (IWT-Vlaanderen). The authors would like to acknowledge the support of Bosal Research for the construction of the different muffler geometries and the financial support of the Institute for the Promotion of Innovation by Science and Technology in Flanders (SBO-IWT 05.0163).

References

[1] Munjal M.L., "*Acoustics of Ducts and Mufflers*", John Wiley and Sons (1987).

[2] Vanelderen B., De Roeck W., Desmet W, "*Influence of Propagation Equations on the Scatter Matrix for Ducts Carrying Non-Uniform Mean Flow* ", AIAA-paper 2010-4011 (2010).

[3] Desantes J.M., Torregrosa A.J., Broatch A., "*Experiments on Flow Noise Generation in Simple Exhaust Geometries*", Acta Acustica united with Acustica, Vol. 87, pp. 46–55 (2001).

[4] Davies P.A.O.L, Holland K.R., "*The Observed Aeroacoustic Behaviour of Some Flow-Excited Expansion Chambers*", Journal of Sound and Vibration, Vol. 239, pp. 695–708 (2001).

[5] De Roeck W., Desmet W., "*Experimental acoustic identification of flow noise sources in expansion chambers*", Proceedings of ISMA 2008, Leuven, Belgium (2008).

[6] Lavrentjev J., Åbom M., Boden H., "*A Measurement Method for Determining the Source Data of Acoustic Two-Port Sources*", Journal of Sound and Vibration, Vol. 183, pp. 517–531 (1995).

[7] Morfey C.L., "*Sound Generation and Transmission Ducts with Flow*", Journal of Sound and Vibration, Vol. 14, pp. 37–55 (1971).

[8] Easwaran V., Gupta V.H., Munjal M.L., "*Relationship between the Impedance Matrix and the Transfer Matrix with Specific Reference to Symmetrical, Reciprocal and Conservative Systems*", Journal of Sound and Vibration, Vol. 161, pp. 515–525 (1993).

[9] De Roeck W., Desmet W., "*Indirect Acoustic Impedance Determination in Flow Ducts Using a Two-Port Formulation*", AIAA-paper 2009-3302 (2009).

[10] Åbom M., Karlsson, M., "*Can Acoustic Multi-Port Models Be Used to Predict Whistling*", AIAA-paper 2010-4009 (2010).

[11] Munjal M.L., Doige A.G., "*Theory of a Two-Source Location Method for Direct Experimental Evaluation of the Four-Pole Parameters of an Aeroacoustic Element*", Journal of Sound and Vibration, Vol. 141, pp. 323–333 (1990).

[12] Åbom M., "*Measurement of the Scattering-Matrix of Acoustical Two-Ports*", Mechanical Systems and Signal Processing, Vol. 5, pp. 89–104 (1991).

[13] W. De Roeck, V. Solntseva and W. Desmet, "*Numerical Methodologies to Predict the Noise Generation and Propagation Mechanisms in Multiple Expansion Chambers*", AIAA-paper 2008-2949 (2008).

[14] Dokumaci E., "*On the Propagation of Plane Sound Waves in Ducts Carrying an Incompressible Axial Mean Flow Having an Arbitrary Velocity Profile*", Journal of Sound and Vibration, Vol. 249, pp. 824-827 (2001).

[15] Lung T.Y., Doige A.G., "*A Time-Averaging Transient Testing Method for Acoustic Properties of Piping Systems and Mufflers*", Journal of the Acoustical Society of America, Vol. 73, pp. 867-876 (1983).

[16] Boonen R., Sas P., "*Calibration of the two microphone transfer function method to measure acoustical impedance in a wide frequency range*", Proceedings of ISMA 2004, Leuven, Belgium (2004).

[17] Venkatesham B., Tiwari M., Munjal, M.L. "*Transmission loss analysis of rectangular expansion chamber with arbitrary location of inlet/outlet by means of Green's functions*", Journal of Sound and Vibration, Vol. 323, pp. 1032–1044 (2009).

[18] Sullivan J.W., Crocker M.J. "*Analysis of concentric tube resonators having unpartitioned cavities*", Journal of the Acoustical Society of America, Vol. 64, pp. 207–215 (1978).